

Aero-acoustic Analysis of Wind Turbines Blades: Turbulent Boundary Layer Trailing Edge Noise

Vasishta Bhargava

Department of Mechanical Engineering, GITAM University, Hyderabad, Telangana.

Dr. Venigalla Hima Bindu

Department of Aeronautical Engineering, GITAM University, Hyderabad, Telangana

YD Dwivedi

Department of Aeronautical Engineering, GITAM University, Hyderabad, Telangana.

Abstract: Numerical aero-acoustic analysis of wind turbine blades is conducted on three different sized machines 350kW, 2MW & 3MW. The turbine blade is considered as independent noise source in atmosphere and sound pressure levels produced from airfoil self-noise are assessed according to the BPM model. This model is semi empirical and predicts the sound pressure levels for 1/3rd octave band frequencies 20Hz – 10kHz range. The frequency spectra of noise mechanism components for untripped boundary layer and directivity pattern as function of observer distance is illustrated. Model sensitivity is calculated using the directivity at several octave band frequencies and observer azimuth positions. The total sound pressure levels for the turbines are compared with theoretical predictions.

Keywords: Sound pressure level, Airfoil, Boundary layer, Angle of Attack, Directivity, Reynolds number, Strouhal number, Mach number. Center frequency,

I. INTRODUCTION

Wind turbine blades radiate noise due to airfoil surface known as self-noise when subjected to different operating conditions. The geometry of the structure is responsible for noise production coupled with atmosphere. The noise levels produced range from few dB in quiet bedroom to few hundreds of dB comparable to helicopter and jet aircraft. Unwanted sound from machines are termed as ‘noise’ and noise produced from wind turbines depend upon the location or surrounding environmental conditions and landscape. The objective of the study is to numerically evaluate sound pressure levels from wind turbine according to the semi-empirical noise models developed during 1900s by group of researchers at the NASA Langley research center. This model predicts the magnitude of rotational noise from wind turbines and similar to that produced from propellers, compressors etc. Mainly the turbulent boundary layer trailing edge noise mechanism from the blades of wind turbine is analyzed and compared for different size turbines.

II. MODEL DESCRIPTION

The aero-acoustic model was developed by Brooks, Pope & Marcolini (1989) at the NASA Langley research center. It considers several noise sources from the airfoil itself in addition to the noise from the atmospheric turbulence experienced at the turbine. The model predicts the sound pressure levels due to the pressure side, suction side of the blade airfoil elements and the separation stall noise at the stalling angle of attack on the blade. The physical characteristics of the airfoil such as the thickness distribution, twist, trailing edge bluntness and its angle as well as the blade tip sections affect the magnitude of sound pressure level. The model uses boundary layer phenomenon to analyze the flow characteristics around the blade airfoil surface for environmental parameters such as the wind velocity, m/s. The different noise sources in this model are

- Turbulent boundary layer trailing edge noise
- Inflow turbulence noise
- Tip noise
- Trailing edge bluntness noise

The characteristic of turbulent boundary layer noise uses the suction side, pressure side and separation stall (angle dependent noise) that contribute towards the total noise level. In order to assess the sound pressure levels, the flow conditions around the airfoil surface, source and receiver positions and also the numerical assumptions were considered to quantify the sound pressure levels. The distance between source and receiver, receiver height above the ground, wind shear, wind speed, wind direction and physical size of the machine under assessment are factors which affect the sound pressure levels. Brookes Pope and Marcolini [1] measured the surface pressures in order to predict the TBLTE convected from the free field pressure based on the edge scatter formulation proposed by Ffwocs Williams and Hall [1-4] which considers the boundary layer thickness, δ . The results from the overall sound pressure level were scaled to the dependence of fifth power of velocity. The turbulence in boundary layer was characterized as the discrete “hairpin” filament structures in the study by Schlinker and Amiet [3] however, the results had drawbacks related to angle of attack and velocity trends with respect to the measurements. The Reynolds number is required to scale the boundary layer thickness and boundary layer displacement thickness around the surface of the airfoil, while the Mach number, M is dependent upon the relative velocity seen by the blade element and the speed of sound constant, c , 343 m/s. In addition to above physical quantities, the Strouhal number establishes the relationship between the frequency range of interest or $1/3^{\text{rd}}$ octave band center frequency and boundary layer displacement thickness, δ^* , the oncoming free stream velocity, U , m/s. at which the sound pressure levels are calculated.

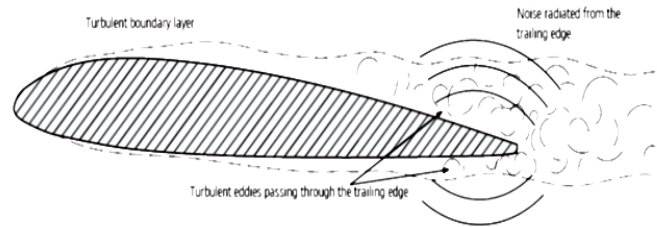


Figure 1 Depiction of boundary layer & TBLTE noise source [9]

The analytical equations [1, 3, 4, 8] of the model for evaluating the sound pressure level from the contributing pressure, suction, separation stall noise and the total TBLTE noise are

$$SPL_p = 10.\log_{10} \left[\frac{\delta_p^* M^5 L D_h}{r_s^2} \right] + A \left[\frac{St_p}{St_1} \right] + [K1 - 3] + \Delta K1 \quad (1)$$

$$SPL_s = 10.\log_{10} \left[\frac{\delta_s^* M^5 L D_h}{r_s^2} \right] + A \left[\frac{St_s}{St_1} \right] + [K1 - 3] \quad (2)$$

$$SPL_{\alpha} = 10.\log_{10} \left[\frac{\delta_{\alpha}^* M^5 L D_h}{r_s^2} \right] + B \left[\frac{St_{\alpha}}{St_2} \right] + K2 \quad (3)$$

$$SPL_{Total} = 10.\log_{10} \left[10^{\frac{SPL_p}{10}} + 10^{\frac{SPL_s}{10}} + 10^{\frac{SPL_{\alpha}}{10}} \right] \quad (4)$$

The Strouhal number and Reynolds number definitions are given by

$$St_p = \left[\frac{f \delta_p^*}{U} \right]; St_s = \left[\frac{f \delta_s^*}{U} \right]; St_1 = [0.02M^{-0.6}]; St_{avg} = \left[\frac{St_1 + St_2}{2} \right] \quad (5)$$

$$Re_p = \left[\frac{\delta_p^* U}{\nu} \right]; Re_c = \left[\frac{U c}{\nu} \right]; \quad (6)$$

The spectral shape functions for the model are denoted by A & B while amplitude correction and adjustment functions are given by K1, K2 and $\Delta K1$ respectively and act as the boundary conditions for the airfoil surface. The following are the set of equations used in the model development for the analysis of boundary layer characteristic on the airfoil surface. The spectral scaling relates the Strouhal numbers, chord wise Reynolds number and Reynolds number dependent upon the boundary layer displacement thickness, δ^* . ν is the viscosity of air at standard atmospheric conditions. The interpolation factor was used to scale the spectral function at each point along the blade span segment length and also to check for the crossing of critical or reference Reynolds number criterion and angle of attack at which stalling occurred.

$$A_R(\alpha_0) = \frac{-20 - A_{\min}(\alpha_0)}{A_{\max}(\alpha_0) - A_{\min}(\alpha_0)} \quad (7)$$

Where, $a = \left| \log \left(\frac{St}{St_{peak}} \right) \right|$ $b = \left| \log \left(\frac{St_2}{St_1} \right) \right|$. The result for the above interpolation function can be expressed as

$$A(a) = A_{\max}(a) + A_R(\alpha_0) |A_{\max}(a) - A_{\min}(a)| \quad (8)$$

Similarly for the spectral function B, the equations are expressed accordingly

$$B_R(b_0) = \frac{-20 - B_{\min}(b_0)}{B_{\max}(b_0) - B_{\min}(b_0)} \quad (9)$$

$$B(b) = B_{\max}(b) + B_R(b_0) |B_{\max}(b) - B_{\min}(b)| \quad (10)$$

The directivity functions of the model are divided into high & low frequency zones of operation and depend upon the position of receiver. Since the position of observer and noise source is not constant correction factors had to be applied in the shifted coordinate system of the turbine. The directivity angles are determined in the shifted coordinate system in order to capture the convective amplification of non-stationary noise source relative to the receiver. The directivity function is dependent upon the position of receiver relative to trailing or leading edge of airfoil. The noise sources [4].are produced from the trailing edge except for the inflow turbulence which originates from leading edge of airfoil. For a wind turbine located in plain land, the shadow zone is observed due to the presence of obstacles where waves fail to propagate. The amplitude of sound waves is considerably reduced in those zones. The acoustic waves are also propagated at a narrow angle due to atmospheric refraction phenomenon and diffraction around the objects.

$$D_H(\theta, \phi) = \frac{2 \sin^2(\frac{\theta}{2}) \sin^2(\phi)}{(1 + M \cos \theta)(1 + (M - M_c) \cos \theta)^2} \quad (11)$$

$$D_L(\theta, \phi) = \frac{\sin^2(\theta) \sin^2(\phi)}{(1 + M \cos \theta)^4} \quad (12)$$

The boundary layer thickness parameters at the trailing edge are obtained from curve fitting expressions for the experimental data [1] for NACA symmetric airfoil at zero and non-zero angle of attack conditions. These are determined for both the pressure side and suction side when the boundary layer is attached, separated near the trailing edge and separated sufficient distance upstream to produce stall [11, 12]. The boundary layers were assumed to be tripped and untripped depending on degree of smooth and clean surfaces on the airfoil. The tripped conditions are achieved by random distribution of grit in the strips from the leading edge ~20% of chord. The thickness of boundary layer was found to decrease with increasing Reynolds number for both tripped and untripped conditions. Boundary layer thicknesses for tripped conditions are fully turbulent while for untripped cases it remained in laminar or transitional states even for lowest Reynolds number. The following are the set of equations [1] for zero angle of attack and non-zero angle of attack conditions

$$\frac{\delta_0}{c} = 10^{[1.657 - 0.9045 \log R_c + 0.0596 (\log R_c)^2]} \quad (13)$$

$$\frac{\delta_0^*}{c} = 10^{[2.0187 - 1.5287 \log R_c + 0.1059 (\log R_c)^2]} \quad (14)$$

$$\frac{\delta_0}{c} = 10^{[0.2021 - 0.7079 \log R_c + 0.0404 (\log R_c)^2]} \quad (15)$$

For the pressure side the boundary layer equations are same for tripped and untripped conditions and a function of Reynolds number for non-zero angle of attack on airfoil.

$$\frac{\delta_P}{\delta_0} = 10^{[-0.04175 \alpha + 0.00106 \alpha^2]} \quad (16)$$

$$\frac{\delta_p^+}{\delta_0^+} = 10^{[-0.04932\alpha + 0.00113\alpha^2]} \quad (17)$$

$$\frac{\delta_s}{\delta_0} = 10^{[-0.04509\alpha + 0.000973\alpha^2]} \quad (18)$$

The suction side boundary layers expressions for non-zero angle of attack and untripped condition are given by

$$\frac{\delta_s}{\delta_0} = 10^{[0.03114\alpha]} \text{ for } 0 \leq \alpha \leq 7.5 \quad (19)$$

$$0.0303 \cdot 10^{[0.2336\alpha]} \text{ for } 7.5 \leq \alpha \leq 12.5$$

$$12.10^{[0.258\alpha]} \text{ for } 12.5 \leq \alpha \leq 25$$

$$\frac{\delta_s^+}{\delta_0^+} = 10^{[0.0679\alpha]} \text{ for } 0 \leq \alpha \leq 7.5 \quad (20)$$

$$0.0162 \cdot 10^{[0.2066\alpha]} \text{ for } 7.5 \leq \alpha \leq 12.5$$

$$52.42 \cdot 10^{[0.258\alpha]} \text{ for } 12.5 \leq \alpha \leq 25$$

$$\frac{\delta_s}{\delta_0} = 10^{[0.0559\alpha]} \text{ for } 0 \leq \alpha \leq 7.5 \quad (21)$$

$$0.0633 \cdot 10^{[0.2157\alpha]} \text{ for } 7.5 \leq \alpha \leq 12.5$$

$$14.977 \cdot 10^{[0.258\alpha]} \text{ for } 12.5 \leq \alpha \leq 25$$

From the directivity function, it can be noted that the angles, θ and ϕ are inclined with x and y axis directions in the coordinate system which represent the angle between observer on ground and the blade axis in the rotor plane of rotation and rotor axis of turbine. The term M_c denotes the convective Mach number and used to assess the amplification of radiated sound from the blade airfoil surface element. The low frequency directivity functions were applied for condition if the corrected angle of attack exceeds 12.5° or peak value of amplitude function K2 defined by angle definition for zero and non-zero angle of attack expressed as function of Mach number. For this condition, the chord wise Reynolds number [1, 10] is taken to be three times the initial Reynolds number with spectral function B replaced with A' for the separated stall noise i.e. SPL_α . Further, the SPL (sound pressure level) for both pressure and suction side is calculated using the boundary layer and displacement thickness from only the suction side due to reversal of pressure distribution on airfoil surface, as result of large non-zero angle of attack conditions. The spectral amplitude functions K1 and K2 and adjustment function $\Delta K1$ are expressed in terms of chord wise Reynolds number, Reynolds number dependent on the pressure side displacement thickness, angle definitions which relate with convective Mach number. The Strouhal number dependence on angle of attack is given by relation

$$St2 = St1 \text{ for } \alpha < 1.33$$

$$St2 = St1 \times 10^{0.0054(\alpha - 1.33)^2} \text{ for } 1.33 < \alpha < 12.5$$

$$St2 = 4.72 \times St1 \text{ for } \alpha > 12.5$$

Interpolated values at each point on the airfoil surface are obtained by comparing with the reference Reynolds number and corrected angle of attack. The reference Reynolds number is defined in the model as

$$Rc_0 = 10^{(0.215\alpha + 4.978)} \text{ for } \alpha < 3 \text{ deg}$$

$$Rc_0 = 10^{(0.12\alpha + 5.263)} \text{ for } \alpha > 3 \text{ deg}$$

Ratio of boundary layer thickness to boundary layer displacement thickness, $R = \frac{\delta}{\delta^+}$ this ratio is utilized to calculate the boundary layer displacement thickness at each blade segment iteratively for all the azimuthal and observer positions for both suction and pressure sides of airfoil. The output from the boundary layer and displacement thickness is required to evaluate the Strouhal number [1] as well as the sound pressure level from pressure, suction and separation noise components. The peak Strouhal number is used to calculate limiting values for the spectral functions A and B used in the analysis. Better results for boundary layer ratios are obtained if average of Strouhal numbers are considered than individual values. The ratio of boundary layer thicknesses indicates the relative sound intensity radiated from the airfoil trailing edge and varies proportionally the fifth power of Mach number, inversely related with square of the distance between the source and receiver.

III. METHODOLOGY

Table 1: Turbine configurations

Parameter	350kW	2 MW	3 MW
Cone angle, deg	0	0	0
Tilt angle, deg	4	3	3
Hub height, m	45	65	80
Radius, m	17	36.5	46.5
Rated speed, rpm	24	17	15
Max twist, deg	15	13	13
Max chord, m	1.085	3.22	3.96

The coordinate systems applied for wind turbine models are 2D transformation matrices a_1, a_2, a_3, a_4 at blade chord, hub center, tower base, tower top. They represent the translation, scaling and rotation of structural variables of the turbine blade viz. twist, chord, cone and tilt angle and blade span segment length to calculate relative velocity seen by the blade element. This enables to compute the coordinates of a point on each blade in coordinate system 1 and utilizes the vector addition of transformation matrices present in coordinate system 3 & 2 respectively. Further, the unsteady BEM simulation model from M. Hansen (DTU) [11] considers the dynamic parameter like the yaw angle which account for the yaw phenomenon by the turbine when there is change in direction of wind. The relative velocity seen by the blade is therefore the vector addition of relative wind velocity components, rotational speed of the turbine and the induced velocity seen by the blade segment. The observer position is first defined in the Cartesian coordinate system with respect to tower base or ground, and converted to spherical coordinate system. This is done in order to capture the varying azimuth angle between the observer position and a point on the rotating blade and since sound waves travel as spherical waves in near field which exhibit spherical spreading phenomenon. This point exists in the local blade coordinate system of the turbine. The relative coordinates of point obtained in the local coordinate system is converted back to observer position in spherical coordinate system. The directivity angles are depicted in the following fig 2. They are defined by the angles θ and ϕ , the airfoil is shown as flat plate that moves in rectilinear motion.

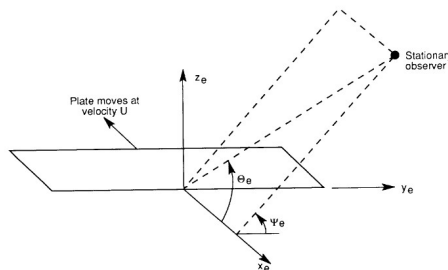


Figure 2: Definition of Coordinate system for Directivity angles [1]

The high and low frequency directivity functions are applied for checking the criterion of chord wise Reynolds number with non-zero angle of attack. In fig 3 the A weighting filter is calculated for 1/3rd octave band center frequency range and used to calculate the A weighted sound pressure or power levels from a point source. It is noted that the results from Wei Zhu [2] were compared with the X-foil method (Mark Drela et al) for correlating the measurements of boundary layer thickness and validation of the sound pressure levels. The numerical simulations were conducted in GITAM University computational lab on two 4GB RAM PC with high end processing power (3GHz) for different observer and source configurations. The results are presented with varying observer distances from source location and found that noise emission levels decrease by 6dB for every doubling of the observer distance.

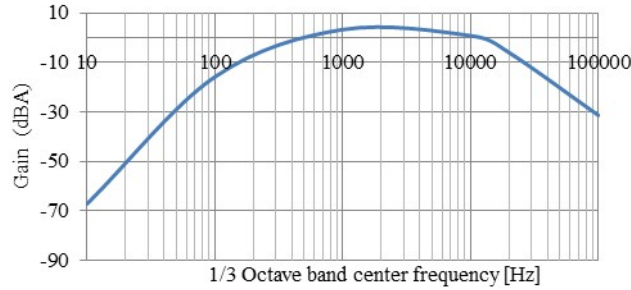


Figure 3 A weighting filter sound pressure level reference (dBA)

IV. RESULTS AND DISCUSSION

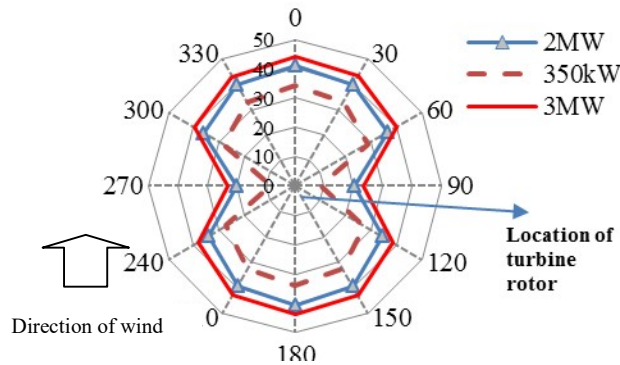


Figure 4 Comparison of Sound Pressure Levels [dB] for 3 machines

The sound directivity as observed from different positions of a receiver is shown in fig 3. It is computed for wind velocity of 8 m/s. It can be noted that large size machines tend to produce higher noise levels in the MW range, while for the kW size of order 10kW – 400kW machines inherently lower values. At each frequency range of interest the turbine produce different comparable sound pressure levels. The fig 4 shows directivity of 2MW machine at lower frequencies. Further from fig 5 it can be seen that the separation stall noise is higher at lower frequencies and comparable with suction side values for small size machines. This trend is not observed for MW size machines, in which the suction side noise dominates over the separation stall noise mechanism.

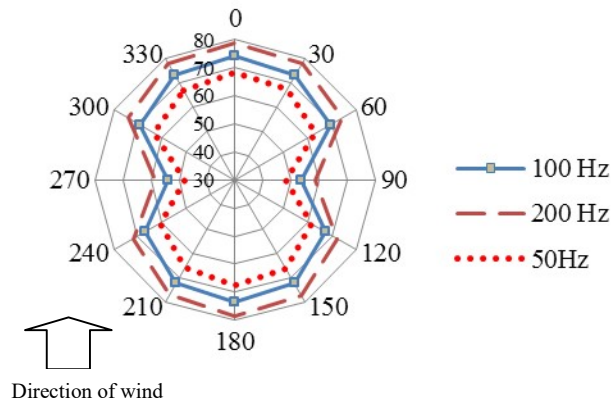


Figure 5 Comparison of directivity sound power levels (dB) [Lw] for 2 MW turbine at 50Hz, 100Hz & 200Hz

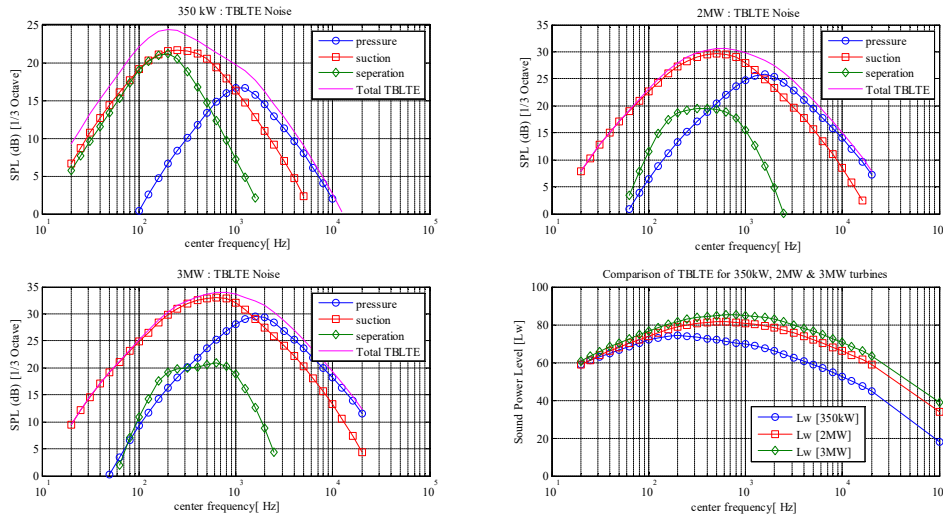


Figure 6: 1/3 Octave band; TBLTE Sound pressure & power levels for 350kW, 2MW, 3MW turbines

The geometric spreading describes about the attenuation of sound levels [7] and characterized with spherical and cylindrical propagation. Sound intensity refers to average amount of sound energy transmitted per unit time through a unit area in a specified direction. The sound levels tend to decrease with doubling distance. In case of spherical, it is $\sim 6B$ and occurs rapidly with a higher attenuation, while for the cylindrical spreading; it is $\sim 3dB$ per doubling distance and usually occurs in downwind direction and for distances greater than 750m from the source (Hubbard & Shepherd, 1991) [13]. They are also often coupled with low level jet where the wind speed ranging from 10-20m/s.

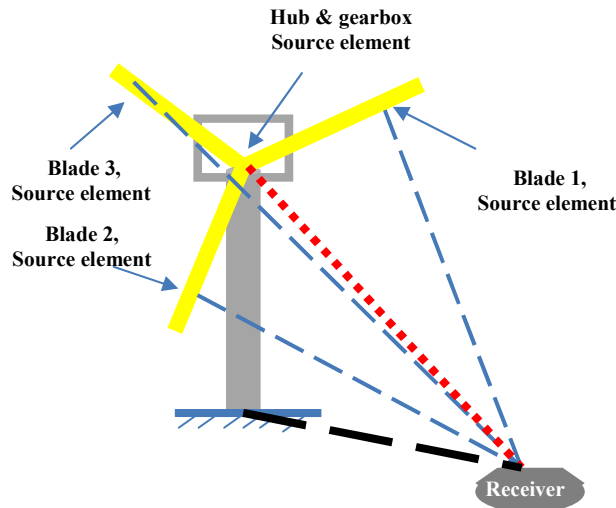


Figure 7 Schematic diagram of perceived acoustic source levels from a wind turbine in open space

The fig 8 shows the sound characteristic as perceived acoustic level from a receiver located at a height above the ground. The ground surface roughness is important to analyze the sound propagation in the atmosphere and resulting wind shear due to velocity gradients within the atmospheric boundary layer. Further, atmospheric conditions such as the temperature, wind speed and size of obstacles also influence the sound rays to travel in all directions. It is observed that the sound rays diverge in upward direction for upwind conditions while the waves deflect downward in downwind conditions and treated as point source for distances less than 750m [13].

Table 2: Summary SPL data for 3 machines

Machine	Sound pressure level (dB) [1/3 Octave]			Receiver position, downwind, m
	Observer Distance, m			
	80	140	200	
350kW	34.27	29.12	23.45	5
2 MW	40.93	35.19	29.86	5
3 MW	44.10	38.81	33.44	5

The rotating blade source elements form an integral part of the aerodynamic noise in particular from the trailing edge of airfoil. The sound power level from total turbulent boundary layer trailing edge source is compared with theoretical approximation as shown in fig 9 for three machines. The geometric divergence from a rotating blade source at 90 deg observer position for 50%, 75 % & 95 % of normalized blade radius are compared and found to be higher for mid span blade section than towards the tip of blade. The reduction in the sound pressure level for distances is of order, ~5-6dB per doubling distance which indicates the spherical spreading for distances less than 750m and upwind direction. Further, the attenuation of sound pressure levels with distance is based on the atmospheric absorption reaching the shadow zone. The attenuation is used to estimate the magnitude of transmission loss which prevails higher in shadow zones and dependent on frequency. The assumed distances at which the receiver is located from the turbines are 80m initially. Later the sound pressure levels are also compared for only one machine, 2MW at different distances of receiver position. The attenuation of sound pressure levels is dependent upon the ground effect where the source is located. It is modeled according to the wind shear exponent for terrain class assumed as presented in table 3.

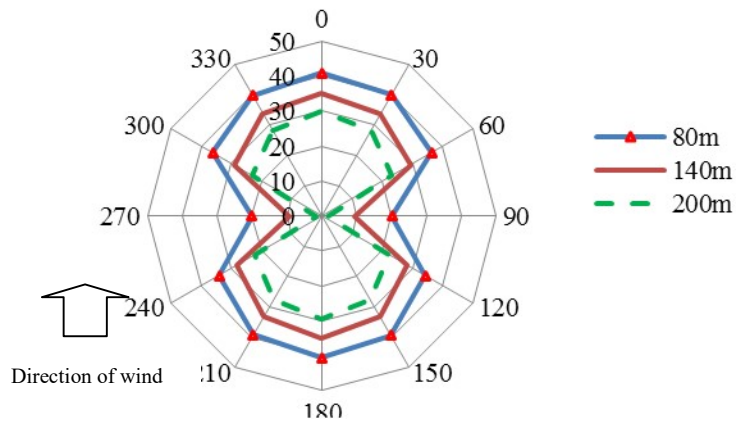


Figure 8 Attenuation of sound pressure level [dB] with distance for 2MW machine

Table 3: Assumptions for atmospheric variables

Parameter	350kW	2 MW	3 MW
Wind shear	0.18	0.13	0.1
Wind speed	8 m/s	8 m/s	8 m/s
Terrain type	Plain land ; Dwellings,	Light vegetation	Near a coast

The sound intensity is calculated using the inverse square law, $I = I_0 \left(\frac{r_0}{r}\right)^2$ [3, 8] where I_0 is the acoustic source level at reference, r_0 is taken to be 1m, r is distance between the source and receiver position. The theoretical approximation of sound power level as function of turbine size is given by relation

$$LwA = 11 \cdot \log_{10} \left(\frac{\text{RatedPower}}{\text{MW}} \right) + 101.1 \text{ dB} [7, 9]$$

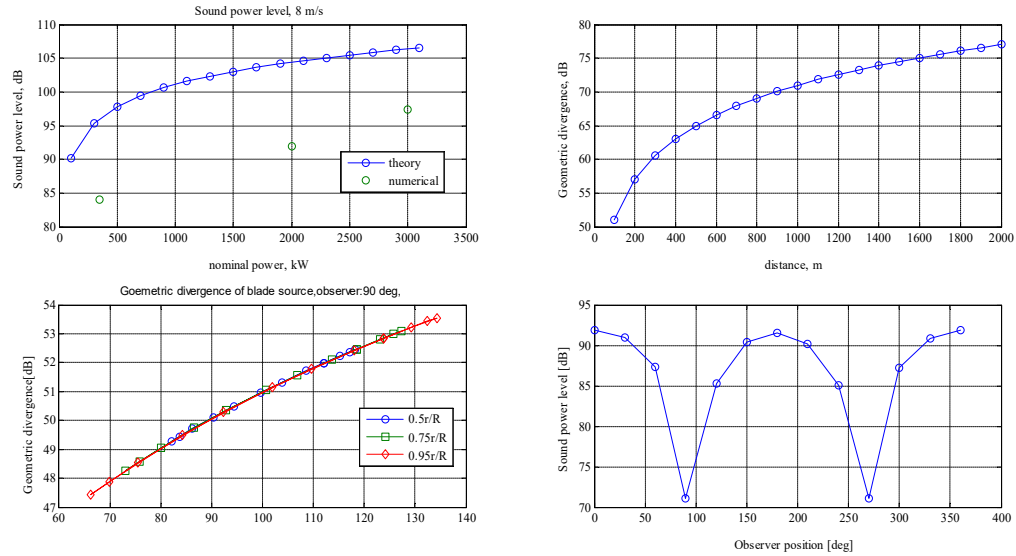


Figure 9: Comparison of numerical results with analytical approximation & Geometric divergence characteristic in dB

V. CONCLUSIONS

The turbulent boundary layer developed due to the trailing edge as noise source mechanism was studied in order to predict the aerodynamic noise radiated for different frequency range components. Trailing edge noise from blade airfoils was found to be dominant at high frequencies only and magnitude of sound pressure levels depend on the angle of attack definitions. The directivity of sound, boundary layer properties and distance between the source and receiver are essential to evaluate the sound pressure levels at different perceived observer positions. The noise intensity is found to decrease higher in cross wind direction of the rotor plane rather than upwind and downwind directions. The model described is applicable to all wind turbines regardless of its size. At low frequencies the separation stall noise is found to be as significant as suction side noise radiation from blades of smaller turbines compared to large MW size turbines. Sound waves are assumed to propagate in atmosphere like optic rays and influenced by the atmospheric conditions. They act as point source or line source depending upon the distance between the source and receiver and the upwind or downwind calculated values.

VI. NOMENCLATURE

- SPL – Sound Pressure Level
- dB – Decibel
- Lw – Sound Power Level
- LwA – A weighted
- BPM – Brooks, Pope, Marcolini
- I - Sound intensity,
- δ_s – Boundary layer thickness on suction side
- δ_p – Boundary layer thickness on pressure side
- δ_0 – Boundary layer thickness at zero angle of attack
- δ_s^* - Boundary layer displacement thickness on suction side
- δ_p^* - Boundary layer displacement thickness on pressure side
- δ_0^* - Boundary layer displacement thickness at zero angle of attack
- θ_0 – Momentum thickness at zero angle of attack
- α – Angle of attack, deg

M, M_c - Mach number and Critical Mach number

Re_c, Re_p – Chord wise and Pressure side Reynolds number

REFERENCES

- [1] Thomas F. Brooks, D Stuart Pope, Michael A Marcolini “Airfoil Self Noise and Prediction” NASA
- [2] Wei Jhun Zhu “Modeling of noise from wind turbines”. June 2004. DTU Wind Energy.
- [3] F.W. Grosveld. “Prediction of Broadband noise from horizontal axis wind turbines” The Bionetics Corporation, Hampton, Virginia.
- [4] P. Moriarty, P. Migliore. “Semi –empirical aero-acoustic noise prediction code for wind turbines” NREL Technical report. NREL/TP-500-34478.
- [5] ManneFriman. “Directivity of sound from wind turbines”. The Markus Wallenberg laboratory for Sound and research.KTH University. Stockholm, Sweden.
- [6] Seunghoon Lee &Seungmin Lee, Soogab Lee. “Numerical modeling of aerodynamic noise in time domain” Aero-acoustics and noise control lab. Seoul National University, Seoul, Republic of korea.
- [7] Moller Henrik, Pedersen, Christian Sejer “Low frequency noise from large wind turbines”. 2011, Aalborg university, Denmark.
- [8] Pieter Dijkstra “Rotor noise and aero-acoustic optimization of wind turbine airfoils”. Delft University of Technology. June 2015.
- [9] Oriol Ferret Gasch. “Assessment, development and validation of wind turbine noise prediction codes”. DTU Wind energy, M-0053, June 2014.
- [10] Charles Ladson, Darrel W Sproles, “Computer Program to obtain ordinates for NACA airfoils”. Langley Research center. Virginia. Computer science corporation, Hampton, Virginia.
- [11] Martin O. L Hansen. “Unsteady BEM simulation model”, DTU Wind Energy.
- [12] Ervin Bossayni, Burton, Sharpe. “Wind Energy Handbook”, Wiley Edition, 2001.
- [13] H.Hubbard, K. Shepherd. “Aero-acoustics of large wind turbines”. Lockheed Engineering Sciences Company, NASA Langley Research Center Hampton, Virginia.